# Structural and optical properties of thermally reduced graphene oxide for energy devices

Ayesha Jamil, Faiza Mustafa, Samia Aslam[†], Usman Arshad, and Muhammad Ashfaq Ahmad[‡]

*Department of Physics, COMSATS Institute of Information Technology, Lahore* 54000, *Pakistan*

(Received 20 January 2017; revised manuscript received 10 May 2017; published online 10 July 2017)

Natural intercalation of the graphite oxide, obtained as a product of Hummer's method, via ultra-sonication of water dispersed graphite oxide has been carried out to obtain graphene oxide (GO) and thermally reduced graphene oxide (RGO). Here we report the effect of metallic nitrate on the oxidation properties of graphite and then formation of metallic oxide (MO) composites with GO and RGO for the first time. We observed a change in the efficiency of the oxidation process as we replaced the conventionally used sodium nitrate with that of nickel nitrate $Ni(NO_3)_2$, cadmium nitrate $Cd(NO_3)_2$, and zinc nitrate $Zn(NO_3)_2$. The structural properties were investigated by x-ray diffraction and observed the successful formation of composite of *M*O–GO and *M*O–RGO ($M$ = Zn, Cd, Ni). We sought to study the effect on the oxidation process through optical characterization via UV-Vis spectroscopy and Fourier Transform Infrared (FTIR) spectroscopy. Moreover, Thermo Gravimetric Analysis (TGA) was carried out to confirm $> 90\%$ weight loss in each process thus proving the reliability of the oxidation cycles. We have found that the nature of the oxidation process of graphite powder and its optical and electrochemical characteristics can be tuned by replacing the sodium nitrate ($NaNO_3$) by other metallic nitrates as $Cd(NO_3)_2$, $Ni(NO_3)_2$, and $Zn(NO_3)_2$. On the basis of obtained results, the synthesized GO and RGO may be expected as a promising material in antibacterial activity and in electrodes fabrication for energy devices such as solar cell, fuel cell, and super capacitors.

**Keywords:** thermal properties of graphene oxide and reduced graphene oxide, optical properties, structural properties, fuel cell, composite materials

**PACS:** 65.80.Ck, 78.67.Wj, 61.48.De, 82.47.Ed **DOI:** 10.1088/1674-1056/26/8/086501

## 1. Introduction

Due to its unique properties of theoretical large surface area (2630 $m^2 \cdot g^{-1}$), high electron mobility ($2 \times 10^5$ $cm^2 \cdot V^{-1} \cdot s^{-1}$), high Young modulus (1.1 TPa), thermal conductivity (5000 $W \cdot m^{-1} \cdot K^{-1}$) and it has optical transmittance (97%) and good electrical conductivity,[1–4] graphene has been the subject of intense research for more than a decade. This single atom thick layer of $sp^2$-bonded carbon material promises to be a material of great choice for a wide variety of applications including supercapacitors,[5] batteries,[6] sensors,[7] nanoelectronics,[8] hydrogen storage,[9] transparent conducting electrodes, solar cells,[10] and medical fields.[11,12] The two-dimensional (2D) monolayer spread with a honeycomb lattice carries the C=C resonance structure with electronic order directly related to its unique electro–chemical and mechanical properties.

Being a material with plethora of applications, the process of development of a cost-effective and mass-produced graphene has seen many variations. In this context, literature reports various methods for the well-controlled production of graphene which include micro-mechanical exfoliation of bulk graphite (scotch tape method),[13] chemical vapor deposition (CVD), and epitaxial growth on nonelectrical surface as like SiC.[14,15] Such techniques although provide precise manufacturing of graphene sheets for device integration but at the same time suffer from the risk of being high cost and low yield. To overcome this challenge, intense research has been underway for a controlled synthesis of high quality graphene through wet chemical treatments of natural flake graphite.[16–18] Graphene is a 2D monolayer of carbon atoms, which has hexagonal structure and there is $sp^2$-hybridization in carbon atom whereas in graphite, graphene layers are bonded by $\pi$–$\pi$ stacking interaction.[11,12] Such processes primarily consist of oxidation of graphite in the presence of chemical oxidizing agents to produce graphite oxide which is further functionalized or intercalated to obtain the desired product of GO as the primary step towards the final reduction to pure graphene.[17] The chemical efficiency of the former process therefore can be considered as a deciding parameter towards the overall production of graphene. The method originally developed Brodie in 1859 who observed the oxidation of graphite in the presence of fuming nitric acid and potassium chlorate as an oxidants.[16] The method was improved by Staudenmaier through the addition of concentrated sulfuric acid to the mixture,[17] which was later on modified by the to-date much widely adopted method of Hummers and Offeman to find a safer alternative for graphene production by replacing the chemical reactants with the ones which aim

[†]Corresponding author. E-mail: saslam@ciitlahore.edu.pk
[‡]Corresponding author. E-mail: maahmad@ciitlahore.edu.pk

© 2017 Chinese Physical Society and IOP Publishing Ltd 

at the *in-situ* production of nitric acid which acts for the intercalation of graphite, through the reaction of $H_2SO_4$ with $NaNO_3$.[18] The reported methodology has gone through various modifications to enhance the overall oxidation efficiency of graphite. At the same time, the process has been investigated for the functionality of graphene oxide due to the reaction-specific unique oxygen containing functional groups which are ultimately thought to influence the optical, electrochemical, and mechanical properties of graphene for a diverse range of applications.[19]

In this study, we aim to report the efficient synthesis of GO by modified Hummer's method and an in-depth study of the effect of various metallic nitrates, including the conventionally used $NaNO_3$ as well as $Ni(NO_3)_2$, $Zn(NO_3)_2$, and $Cd(NO_3)_2$, on the oxidation properties of graphite. The changes in the oxidation level and the functional groups for each reaction process have been identified using various optical and structural characterizations. It is hoped that the results obtained may suggest some useful information about property-dependent functionality of graphene for diverse application including super-capacitors, solar cells, LEDs, etc.

## 2. Materials and methods

Graphite powder was used to synthesize graphite oxide by modified Hummer's method. To do this, a calculated quantity of graphite powder [2.5 g], metal nitrate [1.25 g], and $H_2SO_4$ [57.5 ml] were mixed under continuous stirring in a beaker kept in an ice bath $KMnO_4$ [7.5 g] was gradually added to further control the solution temperature thus allowing it not to exceed 10 °C. Later on distilled water was added to the solution and mixture was heated at 80 °C for 30 mints under continuous stirring followed by the addition of 30% $H_2O_2$ [25 ml] resulting in a yellowish mixture. The GO particulates were separated from the solution and washed in diluted HCL and distilled water to remove sulphate and metallic ions. The graphite oxide thus obtained at the end of the process was dispersed in distilled water and ultrasonicated to allow sheet exfoliation obtain GO. Untreated GO was removed from the suspension by centrifugation until the bottom of the beaker containing the mixture is clear. Three groups of GO were thus prepared using metallic nitrates including $Cd(NO_3)_2$, $Ni(NO_3)_2$, and $Zn(NO_3)_2$. The samples thus obtained were thermally reduced through the temperature treatment at 100 °C to remove the adsorbed moisture and the resulting characteristics were compared.

## 3. Result and discussion

Figure 1 shows that UV-Vis absorption spectra of GO dispersed in deionized water in the ratio of 0.5 mg/10 ml. The data compare the adsorption profiles of GO as a function of wavelength for the samples obtained as a result of reaction with different metallic nitrates. The graph identifies the presence of peak signatures at 234 nm corresponding to the binding energy 5.29 eV associated with the $\pi$–$\pi^*$ transitions of oxygen containing carbonaceous bands such as C=C, C=O, and C–O or the chromospheres and the nanoscale $sp^2$ aggregation.[4,18] The graph also shows a signature of shoulder at 295 nm associated with $n$–$\pi^*$ of aromatic C–C bond thus a confirmation of the presence of electronic conjugation comparable to the widely reported literature data based on graphene synthesis via Hummer's method using conventional $NaNO_3$.[19–22]

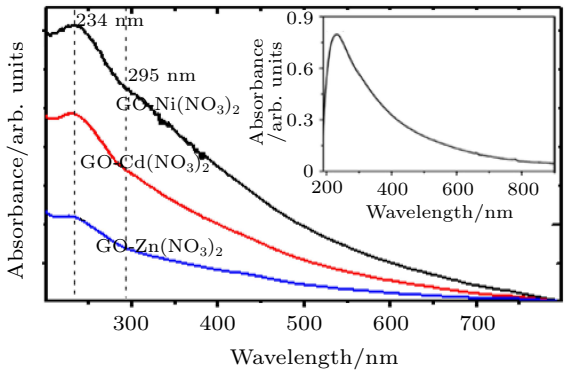



**Fig. 1.** (color online) Absorption spectra of GO by different metallic nitrates and the inset shows the absorption spectrum of the GO synthesized from $NaNO_3$.[22]

The presence of strong absorption at 234 nm has been used as an indicator to hint about the degree of oxidation as well as with the volume density and interlayer thickness of suspended GO flakes graphite.[19,20] A stronger peak for $\pi$–$\pi^*$ electronic conjugation at 234 nm as compared to the one at 295 nm, suggests a high degree of sheet-edge oxidation leading to the resulting product to be highly hydrophilic thereby increasing its solubility in water. The weak signature shown by the reaction of $Zn(NO_3)_2$ suggests that for this sample, the basal plane oxidation was more pronounced as compared to the sheet edge oxidation. The presence of only a single peak in the adsorption spectrum confirms the presence of a few layer graphene as opposed to multi-layered spectra. Moreover, it can be inferred from the spectra that the presence of $Zn(NO_3)_2$ maximally supports the degree of intercalation as opposed to $Ni(NO_3)_2$ for which a multiple layered GO dispersions are obtained as shown by the maximum peak intensity at 234 nm.[19–21] This in turn, results in the largest interlayer distance of GO sheets for $Zn(NO_3)_2$, $Cd(NO_3)_2$ on the other hand, GO by the $Ni(NO_3)_2$ shows more absorbance as compared to the Cd/Zn nitrates. The UV-Vis implications are further supported by the FTIR spectra due to the association of unique functional groups attached with the sample as a result of the competition between two oxidation types.

Figure 2 shows the FTIR spectra for GO obtained at the end of each reaction which indicates the presence of broad peak between 3000 $cm^{-1}$–3700 $cm^{-1}$ associated with the hydroxyl (OH) stretching vibrations adsorbed on the surface of GO to be more pronounced for the case of cadmium nitrate sample thus confirming its strong hydro philicity. The stretch centered around 2360 $cm^{-1}$ indicates absorption by the triple carboxylic acid O–H stretch thus implying the sheet edge oxidation to be more pronounced for $Ni(NO_3)_2$ in comparison to oxidation via $Cd(NO_3)_2$ and $Zn(NO_3)_2$.

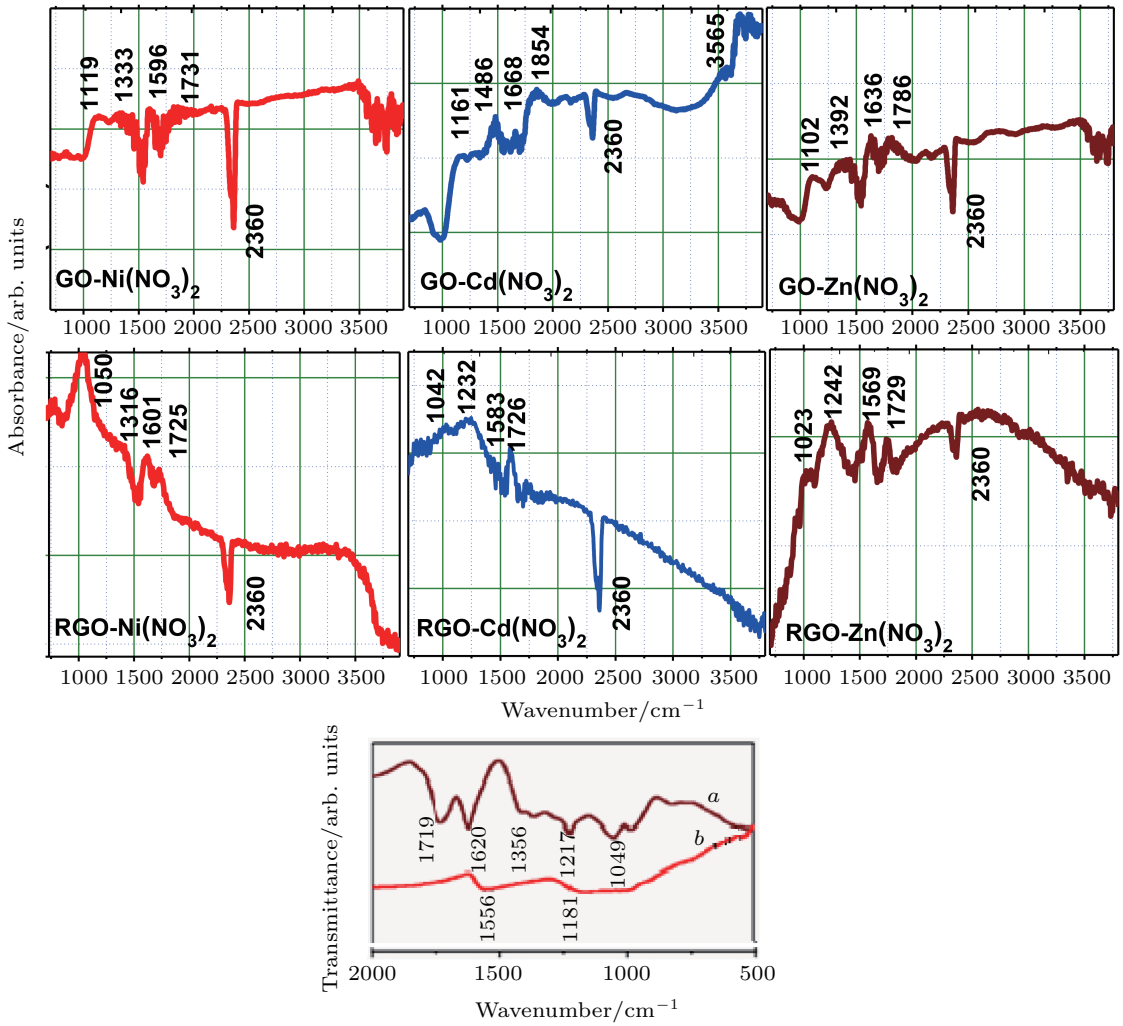



**Fig. 2.** (color online) FTIR absorption spectra of GO and RGO by different metallic nitrates. FTIR spectra of (curve *a*) GO and (curve *b*) RGO by $NaNO_3$.[23]

The FTIR spectra of all GO samples show carbonyl C=O (around 1730 $cm^{-1}$), aromatic C=C (around 1630 $cm^{-1}$), carboxyl O=C–O (around 1330 $cm^{-1}$), and C–O–C (around 1100 $cm^{-1}$) stretching vibration modes. The IR spectra of all RGO samples show peaks around 1730 $cm^{-1}$, 1570 $cm^{-1}$, 1230 $cm^{-1}$, and at about 1050 $cm^{-1}$ which correspond to the aromatic carbonyl C–O, C=C stretch, epoxy C–O stretch, and alkoxy CO respectively.[23] All RGO samples show the blue shift in their IR spectra due to thermal reduction. The associated functional groups show great similarity with those associated with the oxidation through conventionally used sodium nitrate $NaNO_3$ to support oxidation process.[19,23,24] After thermal reduction most of the oxygen containing functional groups are removed as confirmed by the dramatic peak reduction centered around 2360 $cm^{-1}$ and the peaks around 1730 $cm^{-1}$ associated with C=O double bonds.

All the samples of GOs have slight initial mass losses (Fig. 3) at 100 °C which could be attributed to the evaporation of water molecules. The main weight loss (90% to 95%) for GOs by cadmium nitrate and nickel nitrate takes place at 210 °C and 230 °C respectively, is known to be caused by the pyrolysis of the reactive oxygen containing functional groups, yielding $CO_2$, CO, and $H_2O$ vapors.[25,26] But GO by $Zn(NO_3)_2$ has initial mass loss at 100 °C, and second mass loss that was approximately 30% in between 210 °C and 230 °C. GO by $Zn(NO_3)_2$, on the other hand shows a relatively monotonous and slower mass loss was observed and can be attributed to the removal of more stable oxygen functionalities between 230 °C to 800 °C respectively.[27] The relatively slower mass loss experienced by $Zn(NO_3)_2$ sample is

another indicative of increased basal plane oxidation.[19] After the thermal reduction of all samples of GOs, all TGA curves show the same behavior. In contrast, RGO showed much lower weight loss than GO thus thermally stable than GO, indicating a less amount of water absorbed by the RGO than by the GO. There is approximately no weight loss in between 25 °C to 450 °C. After 400 °C to 800 °C significant weight loss was observed corresponding to the removal of more stable oxygen functionalities. It was analyzed that a significant amount of the water and labile oxygen groups were removed by thermal reduction of GO. From the TGA curves however, one can conclude that the three RGO samples have more or less similar stability against thermal decomposition. The four probe DC conductivity measurements of pellets having diameter of $\sim$ 13 mm and thickness $\sim$ 2 mm as a function of temperature were also performed using Keithley 2450 Source Meter and found that conductivity increases as temperature increases which is highly desired in the application of fuel cell.[28] The measured conductivities vary from 0.289 S/cm to 1.082 S/cm for ZnO-RGO and from 0.054 S/cm to 0.983 S/cm for CdO-RGO, and from 0.043 S/cm to 0.798 S/cm for NiO-RGO at 300 °C to 500 °C respectively.

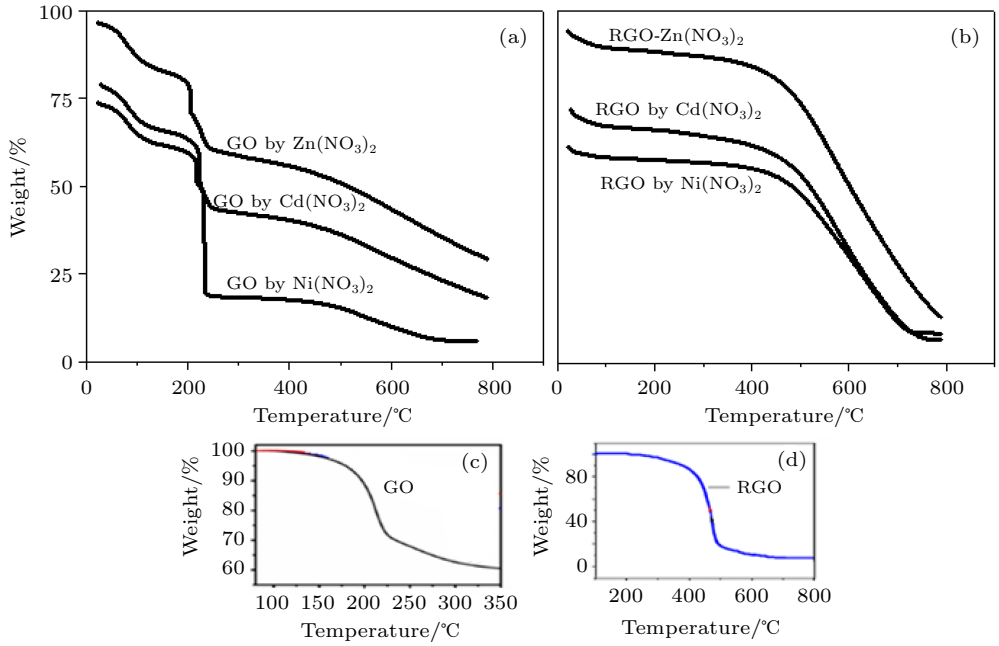



**Fig. 3.** (color online) TGA curves of (a) GO, (b) RGO, and panels (c) and (d) shows the TGA curves of GO and of RGO synthesized from $NaNO_3$ reported in literature,[23,24] respectively.

The XRD pattern obtained for the GO and thermally reduced GO is shown in Fig. 4 which clearly reflects the structural change from GO to RGO. As obvious from (Fig. 4(a)) diffraction peaks for GO-$Zn(NO_3)_2$ indicating the formation of ZnO/GO nanocomposite. The diffraction peaks appearing at 12.6°, 26.4° correspond to (002) and (004) planes, are due to the presence of GO[29] and rest of the peaks at 30.97°, 34.4°, 36.2°, 47.2°, 56.02°, 62.02°, and 68.01° are corresponding to the (100), (002), (101), (102), (110), (103), and (201) planes, respectively, indicating the presence of ZnO. Diffraction peaks for RGO-$Zn(NO_3)_2$ (Fig. 4(a)) at 39°, 54.28°, 62.89°, and 68.09° indexed at (211), (110), (103), and (201) are due to the ZnO and weak peak at 24.03° shows the existence of RGO.[30,31] The XRD analysis shows that the composites obtained were composed of ZnO wurtzite structure with GO and RGO.

The diffraction peak around 11° in XRD pattern of GO-$Ni(NO_3)_2$ (Fig. 4(b)) match up with (111) plane of GO[32,33] and the remaining peaks for both samples around 37°, 43°, 62° correspond to (111), (200), and (220) proving the formation of NiO having cubic symmetry. However, the weak peak at 24.5° for the RGO-$Ni(NO_3)_2$ is the characteristic peak of the RGO along with the signature peaks of Ni nano-particles around 45° (111) and 51° (200).[34] Thus the successful formation of composites of NiO-GO and NiO-RGO is observed. The weak diffraction peaks were also observed around 34° and 42° in all samples which may be due to the residual manganese oxide during reduction of $KMnO_4$.[35–37] From Fig. 4(c), the diffraction peaks around 38° (200), 55° (220), and 69° (222) are in good agreement with the characteristic peaks of the CdO,[38] while prominent peaks at 10.9° (002) and at 26.67° (004) for GO-$Cd(NO_3)_2$ and around 21° (100) for RGO-$Cd(NO_3)_2$ confirms the existence of GO and RGO respectively.[39,40] So, the XRD results confirm the formation of CdO-GO and CdO-RGO composites. The characteristic peaks around 50° and 26° are attributed to the (002) and (004) planes respectively, of the raw graphite in all samples and the diffraction peak located about 19° (101), corresponds to oxidized graphite.[33,41]

Microstrains $\varepsilon$ in all the samples calculated from WH plots are given in Table 1. All values are negative and indicate a compressional strain as a result of nanocomposite formation. Whereas an account of comparison between GO and RGO in all samples shows that the compressional strain in RGO sample is greater than its corresponding GO sample which clearly

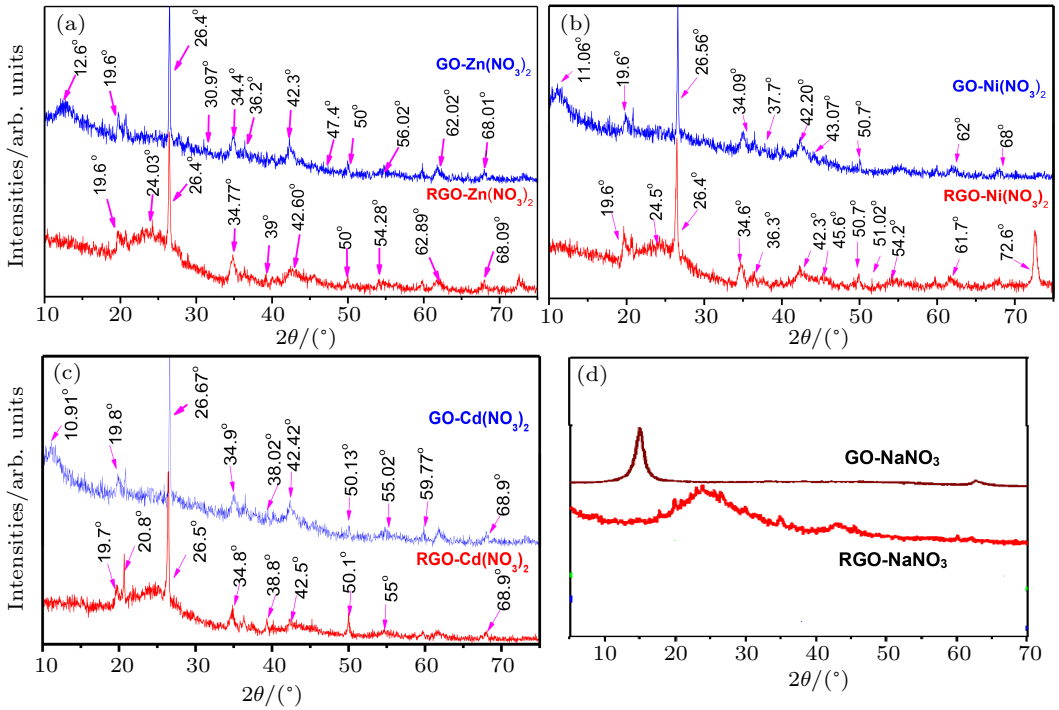



**Fig. 4.** (color online) XRD pattern of (a) GO and RGO synthesized from $Zn(NO_3)_2$, (b) GO and RGO synthesized from $Ni(NO_3)_2$, (c) GO and RGO synthesized from $Cd(NO_3)_2$, and (d) XRD patten of GO and RGO reported in Ref. [23].

**Table 1.** Particle size calculated from Scherer formula (corrected line broadening ) and strain from WH-plots.

| Sample ID | Angle of diffraction $2\theta/(^\circ)$ | Planes | Corrected line nm broadening $D$/nm | Micro strains $\varepsilon$ | Inter planner distance $d$/nm |
|---|---|---|---|---|---|
| GO-$Zn(NO_3)_2$ | 12.08 | [111] | 8 | −0.0485 | 0.70 |
| | 26.6 | [002] | 16 | | |
| | 34.8 | [100] | 10 | | |
| | 42.27 | [200] | 12 | | |
| RGO-$Zn(NO_3)_2$ | 26.6 | [002] | 16 | −11.943 | 0.37 |
| | 34.8 | [100] | 8 | | |
| | 42.27 | [200] | 10 | | |
| GO-$Ni(NO_3)_2$ | 11.11 | [111] | 6 | −0.12857 | 0.79 |
| | 26.6 | [002] | 15.8 | | |
| | 34.8 | [100] | 8.9 | | |
| | 42.27 | [200] | 11.5 | | |
| RGO-$Ni(NO_3)_2$ | 19.3 | [111] | 5.5 | −2.164 | 0.36 |
| | 26.6 | [002] | 15.5 | | |
| | 34.8 | [100] | 9 | | |
| | 42.27 | [200] | 11.6 | | |
| | 72.4 | [201] | 3 | | |
| GO-$Cd(NO_3)_2$ | 9 | [111] | 13 | −0.00954 | 0.80 |
| | 20 | [111] | 6 | | |
| | 26.6 | [002] | 18 | | |
| | 34.8 | [100] | 12 | | |
| | 42.3 | [200] | 5 | | |
| RGO-$Cd(NO_3)_2$ | 20 | [111] | 35 | −0.014 | 0.368 |
| | 26.6 | [002] | 20 | | |
| | 34.8 | [100] | 11.8 | | |
| | 42.3 | [200] | 3.9 | | |
| | 50 | [004] | 21 | | |

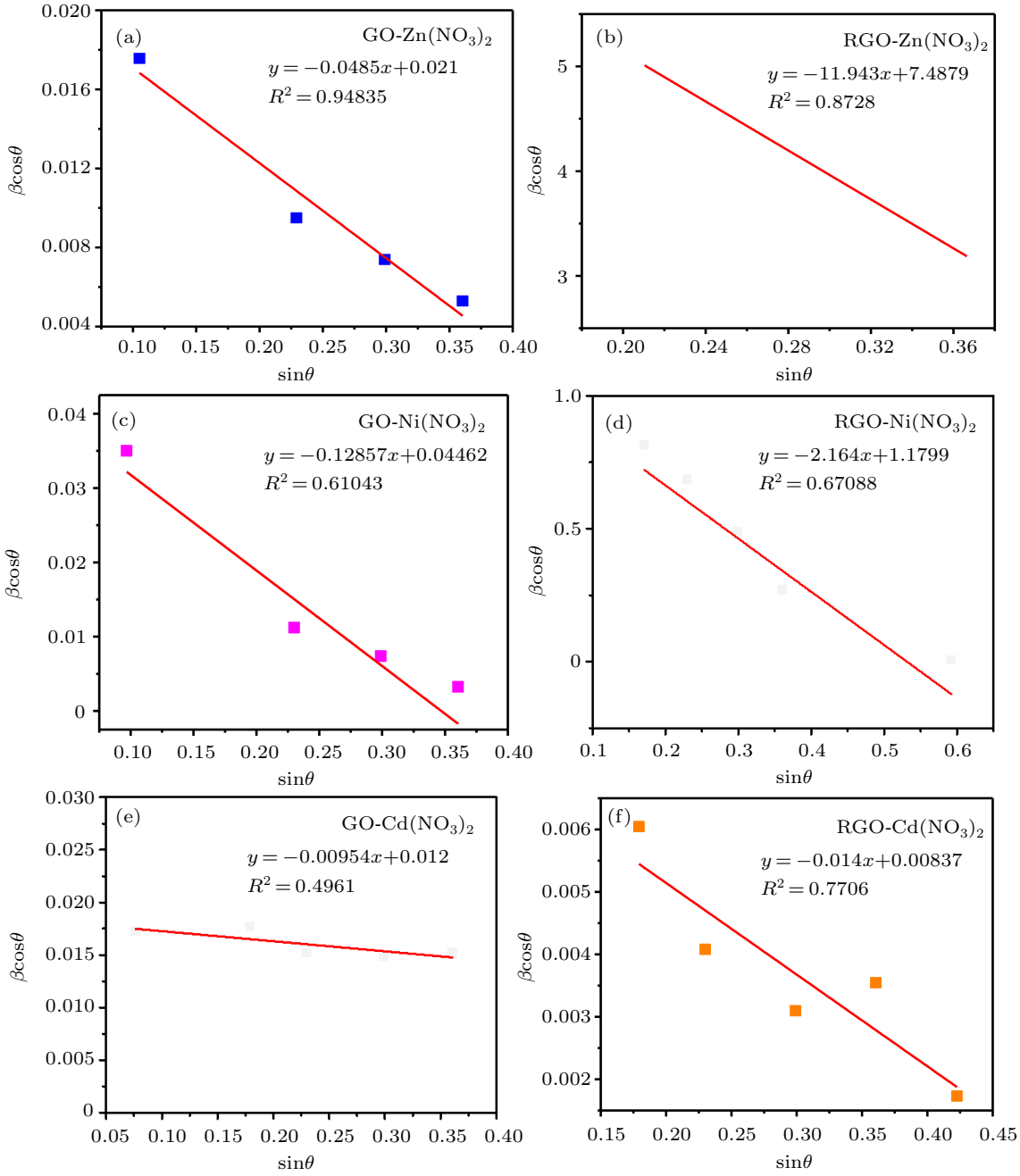



**Fig. 5.** (color online) WH-plots of GO and RGO synthesized from $Zn(NO_3)_2$, GO and RGO synthesized from $Ni(NO_3)_2$, GO and RGO synthesized from $Cd(NO_3)_2$.

shows the removal of oxygen contents during the process of thermal reduction. The highest rate of variation in compressional strain is observed in ZnO-GO and ZnO-RGO samples, the values of $\varepsilon - 0.0485$ and $-11.943$ respectively show the highest rate of oxygen reduction and formation of RGO-composite as compared to other samples. Moreover the inter planner distance $d$ calculated for the characteristics peak of GO at 12.6, 11.06, 10.91 corresponding to 002 for the samples ZnO-GO, NiO-GO, CdO-GO respectively are 0.70 nm, 0.79 nm, 0.80 nm. There is a slight increase in $d$ with slight shift of this peak towards lower angle in all the samples. While the inter planner distance $d$ for the characteristic peak of RGO in all RGO-composite samples corresponding to angles 24.03, 24.5, 24.01 are 0.37 nm, 0.36 nm, 0.368 nm respectively.

## 4. Conclusion

We have compared the oxidation properties of graphite to obtain GO via Hummer's approach but with the variation of nature of metallic nitrates. The optical characterization of GO and RGO confirms the effect of oxidation level of graphite powder changes in Hummer's method for the synthesis of GO due to changing of the metallic nitrate. This will certainly lead to the way of tuning optical properties of the GO/RGO and its uses in energy devices like solar cells, LEDs, and super capacitors. The absorption spectra of the GO are different

and show a variation in oxidation strength of graphite powder. In FTIR characterization, it is clearly seen that the functional groups that are attached with the GO are different as the metallic nitrate was changed. XRD results obtained here confirmed the successful formation of composites of GO/RGO with $MO$ ($M$ = Zn, Cd, Ni). Conductivity measurements show constant decrease (increase) in the resistivity (conductivity) of RGO with the increase in temperature. TGA curves of thermally reduced GO show maximum stability up to 450 °C with 2% to 3% loss in weight only which may be proven as a potential material to find applications in fuel cell and energy devices.

## Acknowledgment

We thankfully acknowledge the financial support for this work as a part of COMSATS IIT Research Grant program (CRGP) under project No. 16-31/CRGP/CIIT/LHR/14/647 & 649.

## References

[1] Tifeng J, Yazhou L, Yitian W, Qingrui Z, Xuehai Y, Faming G, Adam J P B, Jianzhao L, Tingying Z and Bingbing L 2015 *Sci. Rep.* **5** 12451
[2] Nianduan L, Lingfei W, Ling L and Ming L 2017 *Chin. Phys. B* **26** 036804
[3] Zhu Y, Murali S, Cai W, Li X, Suk J W, Potts J R and Ruoff R S 2010 *Adv. Mater.* **22** 3906
[4] Maiti R, Manna S, Midya A and Ray S 2013 *Opt. Express* **21** 26034
[5] Kannappana J J S, Kaliyappanb K, Maniand R K, Samuthira P A, Yange H and Leeb Y 2013 arXiv e-prints 25
[6] Hou J, Shao Y, Ellis M W, Moore R B and Yi B 2011 *Phys. Chem. Chem. Phys.* **13** 15384
[7] Yuyan S, Wang J, Hong W, Jun L, Ilhan A A and Lina Y 2010 *Electroanalysis* **22** 1027
[8] Yuan W, Chen J and Shi G 2014 *Mater. Today* **17** 77
[9] Lee H, Ihm J, Cohen M L and Louie S G 2010 *Nano* **10** 793
[10] Choi H, Kim H, Hwang S, Choi W and Jeon M 2011 *Sol. Energy Mater. Sol. Cells* **95** 296
[11] Yang Y, Asiri A M, Tang Z, Du D and Lin Y 2013 *Mater. Today* **16** 365
[12] Randviir E P, Brownson D A and Banks C E 2014 *Phys. Chem. Chem. Phys.* **16** 4598
[13] Bonaccorso F, Lombardo A, Hasan T, Sun Z, Colombo L and Ferrari A C 2012 *Mater. Today* **15** 564
[14] Wang Y B, Yin W H, Han Q, Yang X H, Ye H, Lü Q Q and Yin D D 2017 *Chin. Phys. B* **26** 028101
[15] Park S and Ruoff R S 2009 *Nat. Nanotechnol.* **4** 217
[16] Marcano D C, Kosynkin D V, Berlin J M, Sinitskii A, Sun Z, Slesarev A, Alemany L B, Lu W and Tour J M 2010 *ACS Nano* **4** 4806
[17] Gengler R Y N, Spyrou K and Rudolf P 2010 *Appl. Phys. D* **43** 374015
[18] Lai Q, Zhu S,Luo X, Zou M and Huang S 2010 *AIP Adv.* **2** 3
[19] Shang J, Ma L, Li J, Ai W, Yu T and Gurzadyan G G 2012 *Sci. Rep.* **2** 792
[20] Huang P, Xu C, Lin J, Wang C, Wang X, Zhang C, Zhou X, Guo S and Cui D 2011 *Theranostics* **1** 240
[21] Omidvar A, RashidianVaziri M R, Jaleh1 B, Partovi Shabestari N and Noroozi M 2016 *Chin. Phys. B* **25** 118102
[22] Sumit S, Trevor A T, Shobha S, Ezana N, Haiyan C and Jianming B 2011 *Appl. Phys. Lett.* **99** 013104
[23] Zhang C, Chen M, Xu X, Zhang L, Zhang L, Xia F, Li X, Liu Y, Hu W and Gao J 2014 *Nanotechnology* **25** 135707
[24] Naebe M, Wang J, Amini A, Khayyam H, Hameed N, Li L H, Chen Y and Fox B 2014 *Sci. Rep.* **4** 4375
[25] Cao H Y, Bi H C, Xie X, Su S and S Li T 2016 *Acta Phys. Sin.* **65** 146802 (in Chinese)
[26] Mahmood N, Zhang C, Yin H and Hou Y 2014 *J. Mater. Chem.* **2** 15
[27] Ji C, Bowen Y, Chun L and Gaoquan S 2013 *Carbon* **64** 225
[28] Wenhan N, Ligui L, Xiaojun L, Weijia Z, Wei L, Jia L and Shaowei C 2015 *Int. J. Hydrogen Energy* **40** 5106
[29] Zhang Y, Xie L Z, Li H R, Wang P, Liu S, Peng Y Q and Zhang M 2015 *Chin. Phys. Lett.* **32** 098103
[30] Yuvaraj H, Walter V and Jae J S 2014 *Electro. Chimica. Acta* **120** 65
[31] Zhigang W, Yong H, Wenlong Y, Mojiao Z and Xiao H 2012 *Sensors* **12** 4860
[32] Dezhi and LidongL L G 2011 *Nanotechnology* **22** 325601
[33] Koushik B, Arnab M, Manish K M and Goutam D 2014 *Langmuir* **30** 3209
[34] Zaien M, Ahmed N M and Hassan 2013 *Mater. Lett.* **105** 84
[35] Ehab S, Moataz M, Rabeay Y A H and Ibrahim M El S 2016 *J. Nanostruct. Chem.* **6** 137
[36] Xiaochang Q, Shijun L, Chenghang Y and Rong C 2015 *Catalysts* **5** 981
[37] Ban F Y, Majid S R, Huang N M and Lim N H 2012 *Int. J. Electrochem. Sci.* **7** 4345
[38] Yongfu T, Yanyan L, Wanchun G, Teng C, Hongchao W, Shengxue Y and Faming G 2014 *J. Phys. Chem. C* **118** 24866
[39] Debarati R C, Chanderpratap S and Amit P 2014 *RCS Adv.* **4** 15138
[40] Gonçalves N S, Carvalho J A, Lima Z M and Sasaki J M 2012 *Mater. Lett.* **72** 36
[41] Vimlesh C and Kwang S K 2011 *Chem. Commun.* **47** 3942